N90-23309

MORE DATA ON (POSSIBLE) GAMMA-RAY (POINT) SOURCES

W. HERMSEN
Laboratory for Space Research Leiden, P.O. Box 9504,
2300 RA Leiden, The Netherlands

ABSTRACT

The "2CG" catalogue of gamma-ray sources was compiled before detailed knowledge was available on the fine-scale structure of the diffuse Galactic gamma-ray emission. Two independent analyses to discriminate sources which are either compact objects or due to very local and strong enhancements in the Galactic cosmic-ray distribution from those which are artifacts due to the clumpy gas distribution are about to be completed: a maximum likelihood analysis and a cross correlation analysis. Arguments are given why differences, and therefore confusion, in the resulting source lists can be expected.
Detailed analysis of all COS-B gamma-ray data on Geminga (2CG195+04), reveals the existence of a drastic spectral break below 200 MeV. A power-law spectrum with index -1.88 fits the data above about 100 MeV to 3.2 GeV, however, there are also indications for a spectral break above these energies. For energies above about 100 MeV no evidence for long-term time variability was found.
The error region of Geminga was searched for a radio counterpart at wavelengths of 90, 49, 21, 6 and 2 cm using the Westerbork Synthesis Radio Telescope and the Very Large Array. So far 16 sources were detected in this error region. In the direction of 1E0630+178, the Einstein X-ray source proposed to be a Vela-like pulsar and the counterpart of Geminga, no radio source was found at 21, 49 and 90 cm with 3σ upperlimits on the flux densities ranging from 0.5 mJy at 21 cm to 4.5 mJy at 90 cm.
Detailed structures in local molecular cloud complexes are sofar only resolved in gamma rays for the closest and most massive complexes, namely those in the Orion-Monoceros and the Ophiuchus regions. For both region, there is circumstantial evidence for gamma-ray emission from molecular gas that was photodissociated after the passage of a SN shell.

I. INTRODUCTION

The increase in average exposure of the galactic plane region by more than an order of magnitude comparing the SAS-II mission with the COS-B mission didnot result in a proportional increase in the number of identified compact objects. The structured diffuse gamma-ray background makes the search for sources difficult, and the relatively large error regions on the source positions render in many cases several candidate-counterpart objects. The improvement in statistics and angular resolution foreseen for the

EGRET data in the same energy range, and the practically new measurements at the adjacent soft gamma-ray energies by COMPTEL, with angular resolution similar to COS-B, but with improved statistics, should achieve a break-through in the study of compact objects and small-scale active regions.

In this paper some results from ongoing detailed analyses of COS-B data will be reported, supplementing results reported in other papers presented during this symposium, and providing some guidance in the early GRO data analysis. Chapter II, with a discussion on the search for Galactic point sources, complements the presentation by Mayer-Hasselwander; chapters III and IV complement the review paper on Geminga (2GC195+04) by Kniffen; chapter V supplements the paper on gamma-ray emission from clouds by Hunter.

II. GALACTIC POINT SOURCES BEYOND THE DIFFUSE EMISSION

Introduction. The correlation between diffuse galactic gamma rays and gas tracers has been studied in great detail by Strong et al. (1988), using the final COS-B database and HI and CO (tracer of the molecular hydrogen distribution) surveys covering the entire Galactic plane. A good quantitative fit to the gamma-ray distribution is obtained using a model in which the detailed structure of the total gas distribution has been folded with a circularly symmetric Galactic cosmic-ray density distribution to predict the gamma-ray distribution. Those features in the gamma-ray data, which are not explained by this model, are due to active regions in which the cosmic-ray density is locally enhanced, or are due to compact objects. A search for these features, would result in an update of the "2CG" gamma-ray source catalogue (Swanenburg et al. 1981), which was esthablished before Galactic surveys of the CO-line emission were available.

Methods. The first attempt to search systematically for such features was undertaken by Pollock et al. (1985a,b) using a maximum likelihood method. However, at that time only a small fraction of the Galactic plane region was mapped in CO, and the analysis was limited to energies above 300 MeV.

Mayer-Hasselwander and Simpson (1988, see also Simpson and Mayer-Hasselwander, 1987, and Mayer-Hasselwander in this volume) presented results from a search for sources in excess to the same model predictions for the diffuse gamma-ray background. They applied the cross correlation analysis of Hermsen (1980) to all gamma-ray data of the Galactic plane region (in three energy intervals: 70-150 MeV, 150-300 MeV, 300-5000 MeV) and to the model predictions to find the excess structures, calibrating confidence intervals with bootstrap sampling. The derived source list is a first attempt to arrive at a final COS-B list.

In Pollock and Hermsen (1990; final paper in preparation) the results from the maximum likelihood analysis of all COS-B data will be presented, applying the analysis to the same three

differential energy ranges, as well as to the total energy range. Furthermore, the analysis has been applied to the data from each single observation period, and to the combined total COS-B sky distribution. The advantages of this approach (in comparison to the correlation analysis) are the following:

(i) the maximum likelihood analysis is performed on the parameters of single events; the events are not sorted in sky bins.

(ii) the analysis of single observations allows the detection of sources which vary over time scales of months to years.

(iii) in the large-scale correlation study of the diffuse Galactic gamma-ray emission only four strong sources have been taken into account (Strong et al. 1988); therefore, it was decided to treat the absolute level of the structured diffuse gamma-ray background as a free parameter for each observation period.

(iv) the likelihood analysis can naturally test the structure of a significant excess above the diffuse gas emission using the single event distribution, to decide whether the data support the presence of one source, or whether more sources are located closely together.

It is evident that the differences in the two appraoches will result in differences between the derived source lists; particularly the conclusions on variable sources and multiple-source structures will differ. Therefore it will be mandatory to perform a detailed comparison between the two sets of results in order to guarantee a usefull input to the GRO analysis.

Example output. In Figure 1 an example of a Log-likelihood ratio map is shown, indicating the weight of evidence (see discussion in Pollock et al., 1985) for a point source in each position in the 20° field-of-view of COS-B during one observation of the Anti-Centre region centered on Geminga, for three energy intervals. Evidently, there remain only two sources above the predicted diffuse emission: Crab and Geminga. The differences in spectral shape are remarkable: The Geminga profiles saturate for the higher energies, while the source barely shows up at low energies; the Crab is clearly most significant at low energies.

A new variable source? As a preliminary result, an interesting example of the degree of "confirmation" and "contradiction" (and therefore confusion) between the results from the two approaches is given: Mayer-Hasselwander and Simpson (1988) published the detection of two new gamma-ray sources at $(l,b)=(324.7°,-6.1°)$ and $(l,b)=(327.2°,-8.7°)$ at significance levels of 4.5σ and 5.0σ, respectively, and both were only seen in the 150-300 MeV energy range. In fact, in their correlation output using all COS-B data, they found one extended excess centered at about $(l,b)=(325.5°,-7.0°)$, which they interpreted as being due to two sources. However, the sources were not resolved in the correlation output, nor was a statistical test applied to the event distribution using a two-sources model. Therefore, the claim that two sources were discouvered, is questionable.

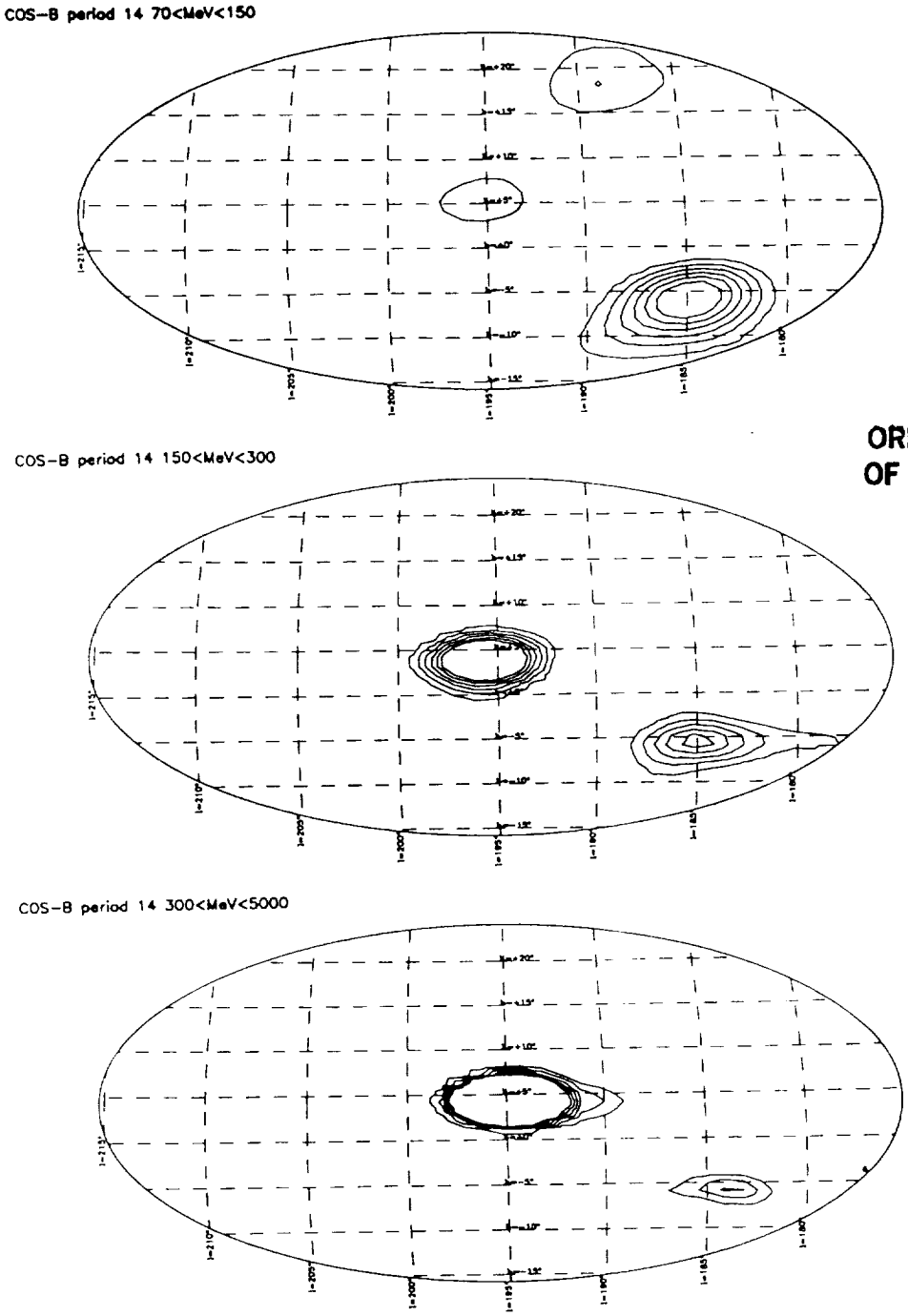

Fig. 1. Log-likelihood-ratio (λ) maps for observation period 14 for three energy intervals. Contour levels: λ = 2, 4, 6, 8, 10, 12.

The general source region around (325.5°,-7.0°) was in the field of view of COS-B during three observations, numbers 7, 33 and 61, at inclination angles 8°, 17° and 9°, respectively. The likelihood analysis for the single observations rendered no detection for periods 7 and 33, but **confirmed** the excess using data from period 61 (see Figure 2). Indeed, for the intermediate

energy range a significant detection can be claimed. Since the latter period was not available when the "2CG" cataloque was generated, this explains the absence of this entry in the catalogue. Preliminary inspection of the likelihood contours in Figure 2, suggests that only one source causes the effect, instead of the claimed two. In conclusion, the likelihood analysis confirms the presence of a significant excess centered at about (l,b)=(325.5°,-7.0°), which, however, seems to be due to a **single time variable source**. More detailed analysis is in progress (Pollock and Hermsen, 1990; full paper in preparation).

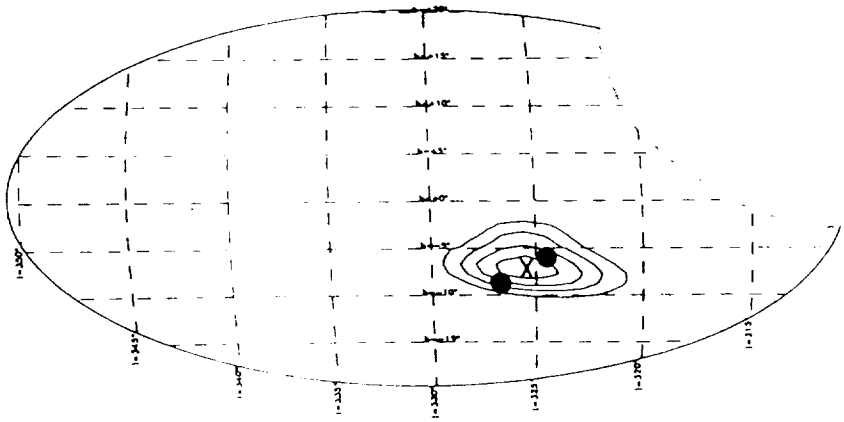

Fig. 2. Log-likelihood-ratio (λ) map for observation period 61 (150-300 MeV). Contour levels: λ= 2,4,6,8. The single evidence for a point source is found at about (l,b)=(325.5°,-7.0°) (indicated by the cross). The two dots indicate the source positions reported by Mayer-Hasselwander and Simpson. The area deleted from the field of view around l=315° at positive latitudes was contaminated by gamma rays coming from the earth.

III. VARIABILITY AND SPECTRAL PROPERTIES OF THE HIGH-ENERGY GAMMA-RAY EMISSION FROM GEMINGA

Introduction. The strong gamma-ray source 2CG195+04 (Geminga) located in the general anti-centre direction, remains an enigma since its discovery in 1975 by the SAS-2 team. Although the relatively small source region (a conservative error radius ≤ 0.4°) has been studied in great detail over the entire electromagnetic spectrum, a definite identification of the source has not been achieved so far.

Most attempts to identify the source concentrated on the X-ray source 1E0630+178, located close to the centre of the error circle. After some earlier claims for identification had to be withdrawn, the proposal by Halpern and Tytler (1988), that 1E0630+178=Geminga is a Vela-like pulsar seems to make a good chance, although they and Bignami et al. (1988) also list some problems with this interpretation (see also the review by Kniffen in these proceedings). If the above identification is correct, Geminga may be characterized by high L_g/L_x and L_x/L_v ratios of the order of 10^3, and the source distance can be as much as 750-1000 pc, based on the X-ray spectrum. Recently, Ruderman and

Cheng (1988) developed for Geminga a model including an evolved, aligned, Vela-like pulsar. A detailed study of the gamma-ray emission from Geminga, its spectral properties and long-term evolution, is essential to provide source parameters which can be tested against this and other models.

Data and analysis. Geminga was in the field-of-view of COS-B five times between 1975 and 1982, out of which initially four periods (14,39,54,64) were selected by Grenier, Hermsen and Hote (1990; full paper in preparation) because of the small source aspect angle (<10°). The energy distribution of the emission between 50 MeV and 5 GeV was analysed for each period independently using the maximum-likelihood analysis developed to describe the Vela pulsar emission (Grenier et al. 1988). An important aspect of this analysis is that the photons are not binned (spatially nor in energy) but treated individually. To describe the bulk of the gamma rays detected in the large field-of-view of COS-B, four different components were considered: 1. an isotropic background emission; 2. the diffuse galactic emission; 3. the point-sources from the Crab pulsar and its nebula; 4. the point-source Geminga supposed to be in the direction l=195.1° and b=4.2° (Masnou et al. 1981). While power-law spectra for the instrumental and galactic background were fitted together with the Geminga spectrum, the stable spectra of the emission from the Crab pulsar and its nubula were taken from the study by Clear et al. (1987). The gamma-ray photons and characteristics of the telescope have been selected from the Final COS-B Database. Details on the maximum likelihood analysis can be found in Grenier et al. (1988). This procedure has the advantage of taking full account of the modest energy and spatial resolutions of the COS-B detector, and that of being sufficiently sensitive to derive spectra for separate observations.

Results. Masnou et al. (1981) combined the data from four observations (0,14,39,54) to determine an average spectrum, applying a conventional method in which the data were binned (Figure 3). The derived spectral shape was consistent with a power-law with index -1.8 between 100 MeV and 3.2 GeV, and it flattened and steepened slightly ($<2\sigma$) at lower and higher energies, respectively. Therefore, as a first approximation, the likelihood analysis was performed to derive the single-power-law spectra that best fit the emission from Geminga in the 50 MeV to 5 GeV interval, for each of the selected observations (14,39,54,64). The results for each period and for the combination of all four observations are listed in Table 1, together with their 1σ statistical errors.

The fit values for the individual observations and for the total spectrum are within their uncertainties consistent with the result by Masnou et al.: Between about 100 MeV and 3200 MeV no long-term variability can be claimed in the spectral indices and in the fluxes inferred from the single-power-law spectra.

TABLE I

Single-power-law fit to the Geminga spectra (50-5000 MeV) for each observation and for all periods together.

Period 14	$(4.66^{+3.01}_{-1.96})10^{-4}E^{-(2.02\pm0.10)}$ ph $cm^{-2}s^{-1}$ MeV^{-1}
Period 39	$(1.19^{+0.84}_{-0.50})10^{-4}E^{-(1.77\pm0.10)}$ ph $cm^{-2}s^{-1}$ MeV^{-1}
Period 54	$(1.41^{+1.32}_{-0.69})10^{-4}E^{-(1.80\pm0.12)}$ ph $cm^{-2}s^{-1}$ MeV^{-1}
Period 64	$(2.06^{+1.42}_{-0.87})10^{-4}E^{-(1.87\pm0.10)}$ ph $cm^{-2}s^{-1}$ MeV^{-1}
All periods	$(2.16^{+0.70}_{-0.52})10^{-4}E^{-(1.88\pm0.05)}$ ph $cm^{-2}s^{-1}$ MeV^{-1}

Closer inspection of the data reveals that below 100 MeV and above 3.2 GeV for all observations the data points are systematically below the one-power-law fit. Thus, there are indications for spectral breaks around 100 MeV and around 3 GeV. The first might explain the failure of soft gamma-ray instruments to detect Geminga, sofar. In Figure 1 we could note that Geminga is already unexpectedly week over the interval 70-150 MeV, possibly due to a strong suppression of the lowest-energy events. It is noted, that flux values assigned to energy bins in a conventional method (data points), depend on the used effective sensitive area for each bin, which is a function of the assumed input spectrum. If a very strong change in spectral shape occurs around 100 MeV (e.g. from index +1.0 to index -2.0), this change can easily be overlooked using the wide energy bins and the assigned flux value for the 50-100 MeV bin will inadvertently be wrong (too high). Therefore, the likelihood analysis has been applied to the single photon spectra, to test a two-power-law spectrum with two independent indices below and above a break energy. Different break energies between 100 and 400 MeV have been tested. The introduction of a second break at higher energies was not attempted since too few photons have been detected from Geminga above 3 GeV (typically less than 10 per observation) to constrain such a fit. Preliminary results indicate a pronounced break and a significant improvement in the quality of the fit (compared to the one-power-law fit) for each observation. The analysis is still in progress, and will also be performed for observation 0 (Grenier, Hermsen and Hote, 1990, in preparation). The first results are shown in Figure 3: The best power-law fits for the data of periods 39 and 54 for some selected break energies. The data support the presence of a break in the Geminga spectrum. The fact that in both cases the change in index becomes more (extremely) drastic selecting a lower break energy, indicates that the real break energy is most likely below 200 MeV.

Discussion. Maximum likelihood analysis of the COS-B Geminga data confirms that the Geminga spectrum from about 100 MeV up to a few GeV is consistent with a power-law spectrum with index of about -1.88. Furthermore, there is no evidence for significant

long-term time variability in flux and spectral shape of the gamma-ray emission in this energy interval. Preliminary results at lower energies provide evidence for a spectral break below 200 MeV. This break might in fact be very drastic (e.g. from index +1 to -1.9), and offers an explanation for the failure to detect Geminga so far at soft gamma-ray and hard X-ray energies. There are hints for a second break (steepening at GeV energies). The odd spectrum, sketched above, differs substantially from the spectrum of the Vela pulsar emission. The latter is particularly interesting, given the proposed identification with a Vela-like pulsar (e.g. Halpern and Tytler, 1988; Bignami et al., 1988; Ruderman and Cheng, 1988).

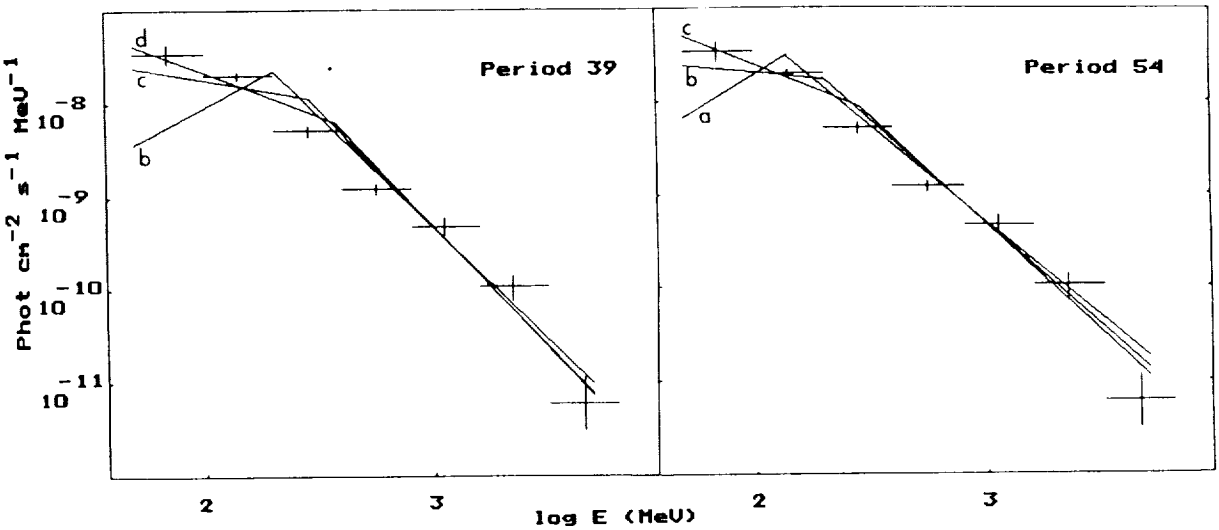

Fig. 3. Two-power-law spectral fits to the Geminga data of observations 39 and 54. Break energies: a) 140 MeV; b) 200 MeV; c) 290 MeV; d) 380 MeV. The data points show the average Geminga spectrum from Masnou et al. (1981) for periods 0,14,39 and 54 (the 50-100 MeV flux value appears now to be wrong since a spectral break was not taken into account for the sensitive area calculation).

IV. ON THE IDENTIFICATION OF THE ENIGMATIC GAMMA-RAY SOURCE GEMINGA: AN EXTENSIVE SURVEY IN THE RADIO BAND.

Introduction. In Chapter III the proposed identification of Geminga with the X-ray source 1E0630+178 was discussed. However, there is no final proof yet of that identification, therefore it is still appropriate to discuss other attempts for identification.

Sieber and Schlickeiser (1982) and Spoelstra and Hermsen (1984) started the search for the Geminga counterpart from the radio band. The latter search (at a wavelength of 21 cm, 1412.0 MHz, using the Westerbork Synthesis Radio Telescope) was the most sensitive one, and a total of 15 sources were detected in the error region with fluxes between about 4 and 50 mJy. Three sources, one of them a quasar, were found to be significantly variable. However, none of these sources appeared to have highly

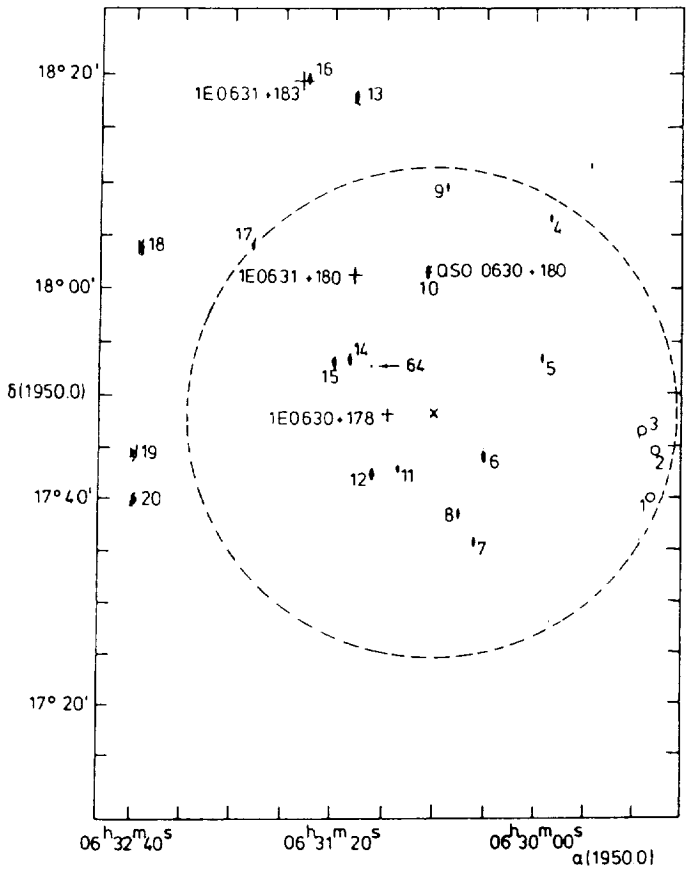

Fig. 4. Contour plot of the field searched at 21 cm wavelength for a possible counterpart of Geminga using data from a 12-h observation in 1982. All detected radio sources are indicated (63W1=1, 63W2=2, etc), including three sources not seen in this observation (o). Also indicated are the best estimate of the Geminga position (x), its error circle (broken line), three Einstein sources (+), and a QSO (63W10). Lowest contour level: 1 mJy. The arrow points at the tiny feature, which is the new source 63W64, discovered at 6 cm wavelength.

anomalous properties at radio wavelengths. Furthermore, Spoelstra and Hermsen reported that no counterpart could be detected in their search for 1E0630+178 with a 3σ upper limit of 0.5 mJy.

New data. Hermsen and Spoelstra (1990) continued this work to obtain an extended and deep survey of this source region in radio. Using the Westerbork and VLA telescopes, data have been collected at 2, 6, 21, 49 and 90 cm, in order to obtain accurate radio spectra and data on time variability of the sources, in the hope to find an anomalous radio source leading to an identification of Geminga. Another point of interest was to search for a radio counterpart of 1E0630+178 at larger wavelengths. Finally, the 1.5m Danish telescope in La Silla, was used to search for optical counterparts of the most interesting sources. In this paper some results are presented from the radio

survey; the analysis of the 2 cm data is still in progress, and a full paper is in preparation (Hermsen et al., 1990).

Results. Spoelstra and Hermsen detected in total 20 sources (source numbers 63W1,...,63W20) at 21 cm, making 12 observations over the years 1980, 1981 and 1982. Figure 4 shows the Geminga error region with the position of all radio sources with flux densities larger than a few mJy. This total sky area was also viewed at 327 MHz and 608.5 MHz (about 90 and 49 cm), and part of the central region inside the error circle also at 4874 MHz (6cm) (centered at the sources 63W6 and 63W15, which showed time variability at 21 cm). Details on these Westerbork measurements and on the VLA observations at 2 cm will be given in the full paper.

It is interesting to report that all sources detected inside the Geminga error circle at 21 cm, have also been seen at 49 and 90 cm, and that no additional detection could be claimed at these longer wavelengths. The weakest source at 49 cm was 63W9 (9.4 ± 1.8 mJy) and the weakest at 90 cm 63W2 (11.2 ± 1.2 mJy). The noise in these radio maps was about 1.5 mJy . Therefore, 3σ upper limits for sources not detected in the Geminga error circle are at about 4.5 mJy at 49 cm and 90 cm. These upper limits apply also to the Einstein X-ray source 1E0630+180, again not seen in our surveys.

Sky regions covering the sources 63W6, 63W14 and 63W15 have been viewed at 6 cm, and the radio spectra of these sources are shown in Figure 5. One should keep in mind that 63W6 and 63W15 showed variability in their flux densities of about 20% at 21cm, therefore average values have been given in Figure 5.

Surprisingly, one new source has been detected at 6 cm, dubbed 63W64 (a high source number, since the new list contains many new sources at longer wavelengths outside the Geminga error region). The flux density at 4874 MHz is (3.2 ± 1.0) mJy, and its position $\alpha(1950.0) = (06^h31^m05.52^s \pm 0.07^s)$ and $\delta(1950.0) = (+17°53'06.8"\pm2.9")$. In fact, inspection of the radio maps at 21, 49 and 90 cm revealed source features at 21 and 50 cm at the position of 63W64, which, however, were below a 3σ detection threshold. In Figure 5 the spectrum of this source is presented as well, and the source position has been indicated in Figure 2.

Discussion. Our extensive survey in the radio band of the Geminga error region reveals a new weak source (63W64), exhibiting a very hard, flat spectrum. An optical counterpart has been found in our measurements from Chile (in collaboration with H. Pedersen) for this source, as well as for some of the other sources. This source, as well as the variable sources reported by Spoelstra and Hermsen (1984) seem to be sufficiently interesting to study them further for a possible identification with Geminga.

If the identification with a Vela-like pulsar (Halpern and Tytler; Bignami et al.) is correct , then of our results only the

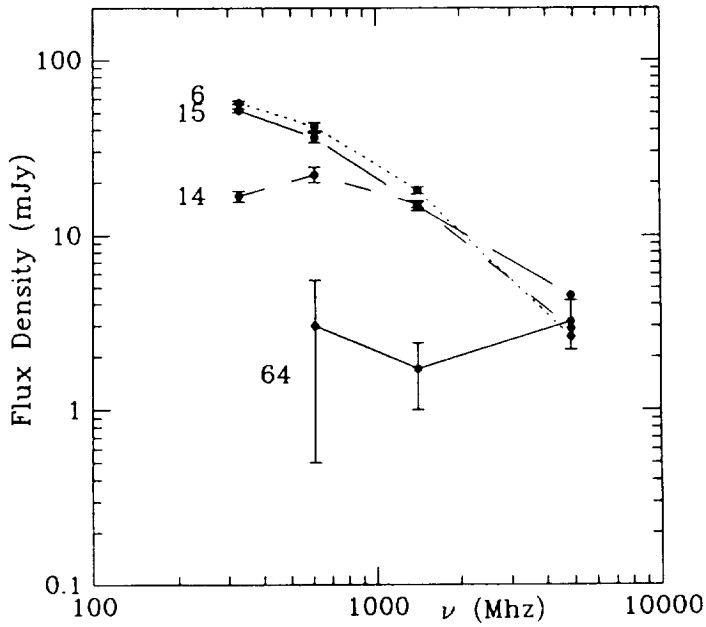

Fig. 5. The measured radio spectra from 90cm to 6cm for the variable sources 63W6 and 63W15, as well as for 63W14 and the new source 63W64. All error bars (1σ) are indicated, except for those at 6cm: the 1 mJy error bar given for 63W64 at 6 cm is typical for the other sources.

radio upper limits (0.5mJy at 21 cm up to about 4.5 mJy at 90 cm) are relevant for the Geminga problem. In this respect it is of interest to note that pulsar models predict a broader radio beam at longer wavelengths. Therefore, the chance to detect the Geminga radio pulsar at longer wavelengths increases for geometrical reasons. A deeper survey in radio is also valuable in order to attempt to detect the predicted weak synchrotron nebula which should surround the Vela-like source, or to improve on our upper limits.

V. CIRCUMSTANTIAL EVIDENCE IN THE OPHIUCHUS AND ORION REGIONS FOR SUPERNOVA SHELLS INTERACTING WITH CLOUDS

Introduction. The Galactic diffuse gamma-ray distribution in the COS-B energy range traces predominantly the product of the interstellar matter (mainly HI and H_2) density and CR density; π^0-decay gamma rays resulting from nucleus (GeV protons)-nucleus interactions, and electron-Bremsstrahlung gamma rays from electron ($\lesssim$1 GeV)-ISM nucleus interactions. The mapping of nearby cloud complexes provides the GRO teams the unique opportunity to study dense active regions in detail to verify these expectations from CR-matter interactions and to search for possible local enhancements in CR density. The complexes in the Orion/Monoceros region were the first for which already with COS-B a detailed correlation study between the gamma-ray data and CO (tracer of H_2) and HI maps could be performed. A good two-dimensional correlation was found between the gamma-ray structures and the total gas distribution, explaining the former in terms of

interactions of the gas with cosmic rays of local density, distributed uniformly in this region (Bloemen et al. 1984).

Early analysis of COS-B data revealed also a significant excess in the direction of the Ophiuchus dark cloud complex (distance about 130 pc) (Swanenburg et al. 1981). Morfill and colleagues (1981) compared the reported flux with mass estimates for the Rho Oph dark cloud and concluded that an enhancement in cosmic-ray density by a factor of about 3 was required, or that the mass and/or distance estimates were wrong. They suggested that the gamma-ray source may be the result of the acceleration of Galactic cosmic rays by an old supernova remnant (the North Polar Spur, Loop I, radius ±115 pc) and its interaction with the Rho Oph cloud. However, after more COS-B data on the region became available, Hermsen and Bloemen (1983) showed that the general structure of the Ophiuchus cloud complex, as delineated in extinction maps and OH data, was in fact resolved in gamma rays. A comparison between the total mass estimated from OH data (Wouterloot 1981) and the gamma-ray flux from the total complex indicated that the measured gamma-ray flux is at most a factor 2 higher than expected, assuming cosmic rays of local density throughout the complex. Given the large experimental uncertainties, this was considered to be insufficient evidence for a local CR enhancement.

Data and results.

Ophiuchus/Upper-Scorpius Region. Recently, a complete CO survey of the Ophiuchus region also became available (de Geus 1988). Figure 6 shows the measured gamma-ray distribution using all available COS-B data on this area for energies between 100 MeV and 6 GeV, as well as the integrated HI column density map and the velocity integrated CO antenna temperature ,W(CO), distribution. The gamma-ray 'beam' is significantly broader than those at radio - and mm wavelengths. Nevertheless, significant structure is visible in the gamma-ray data, showing particularly the molecular cloud complex. Using the $N(H_2)/W(CO)$ conversion factor and the gamma-ray emissivities determined for the solar neighbourhood in the large-scale correlation study by Strong et al. (1988), it can be shown that the gamma-ray intensities predicted for the molecular clouds as traced by CO data are fully consistent with the measurements: There is no indication for an enhancement of cosmic rays inside these clouds. However, the gamma-ray structure appears to be more extended towards somewhat lower longitudes and higher latitudes, already visible in the early map of Hermsen and Bloemen (1983). Therefore, a map of the differences between the predicted structures (using Figures 6b, 6c) and the measurements (Figure 6a) has been determined (Figure 6d). Care has been taken that no significant negative fluctuations are present with respect to the predictions, by adjusting the scaling parameters locally within their uncertainties. Figure 6d shows that at the positions of intense CO emissions the distribution is consistent with zero intensity, but that adjacent to the cloud structures, e.g. at about (l,b)=(351°,18°) and at somewhat higher latitudes, excesses

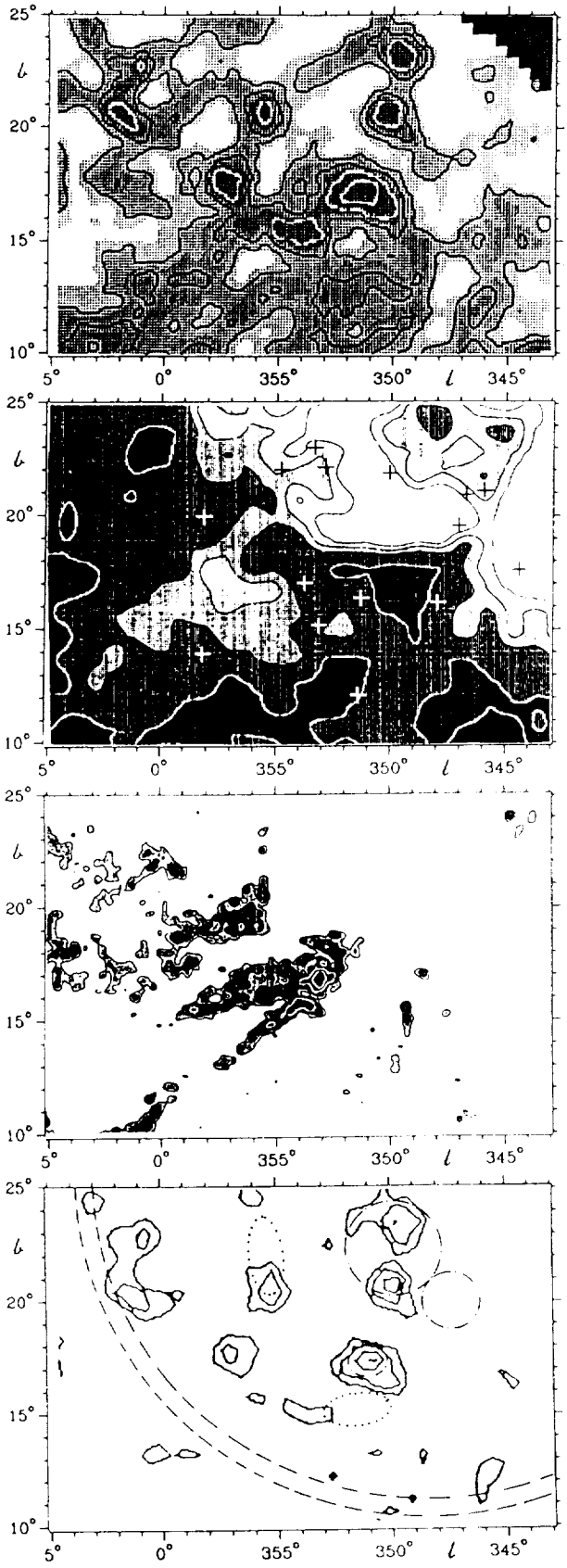

Figure 6 : The Ophiuchus region:

a) Gamma-ray intensities; energies between 100 MeV and 6 GeV. Contour lines at multiples of: $5.x\ 10^{-5}$ ph $cm^{-2}s^{-1}sr^{-1}$; dark area in corner has low exposure.

b) Integrated HI column densities, contour values 12.5, 13.5, 14.5, 17.5, and 20 x 10^{20} cm^{-2}. Positions of the brightest stars (earlier than B2) are plotted as plusses (de Geus 1988).

c) Velocity-integrated CO antenna temperature W(CO) for $-8<v<20$ km s^{-1}. Contour values: 5.0, 20.0, 55.0, 112.5 K km s^{-1} (de Geus).

d) Differences between the observed (a) and predicted diffuse emission based on the HI and CO surveys and the model parameters deduced by Strong et al. (1988). Energies 100-5000 MeV. Contour levels: 8, 13, 18,...x10^{-5} ph $cm^{-2}s^{-1}sr^{-1}$. Dash-dotted circles outline HII regions in Sharpless's catalogue (1959); dotted lines show bright nebula from Lynds's catalogue (1965). Dashed circle segments sketch the expanding shell of radius 40 pc, which overtook the Ophiuchus complex.

remain visible. The first excess coincides with a HII region and with a considerable amount of dust, visible in IR maps (de Geus 1988). Also the excesses at about (l,b)=(350°,22°) are spatially consistent with HII regions and regions with a considerable amount of dust emission with practically no CO present. Again, the reflection nebula at about (l,b)=(355°,22°) is spatially correlated with a dust cloud.

Orion/Monoceros Region. In the Introduction I mentionend that Bloemen et al. (1984) concluded that for the Orion/Monoceros region a good two-dimentional correlation was found between the gamma-ray structures and the total gas distribution. Figure 7 (from Bloemen et al. 1984) shows the similar distributions for Orion/Monoceros as is shown for Ophiuchus in Figure 6. All positive excesses in Figure 7d donot coincide with cloud structures and are located in sky regions in which the CO coverage was poor or missing. However, meanwhile the CO coverage has been completed and particularly one excess structure located at about $(l,b)=(209°,-21°)$ remained. This can be seen in the new map in Figure 8, which is produced similarly as Figure 6d (see also the "finding chart" of Bloemen (1989).

The IRAS data show also in this case enhanced IR emissivity extending over the area of the gamma-ray excess. As will be discussed below, this is another example of a gamma-ray excess adjacent to a molecular cloud, in a region with a considerable amount of dust and HII.

Discussion. Evidently, there appear to be some features in the gamma-ray data of the Ophiuchus/Upper-Scorpius and Orion/Monoceros regions which are not explained by CO and HI structures. Both regions have been studied in great detail earlier, based on measurements at other wavelengths.

Ophiuchus/Upper-Scorpius Region. From a detailed study of the stars and the interstellar medium of the Scorpio-Centaurus OB association, de Geus (1988) recently pointed out that a HI shell (radius about 40 pc) around the stars in Upper Scorpius appears to be created by stellar winds of the early type stars present in Upper Scorpius (indicated in Figure 6b) and by a supernova explosion of a massive star of about 40 $M_\odot$ and about 1 Myr ago. The detailed structure of the interstellar medium, including the elongated CO structures can be explained as being due to the passage of the SN shock (the approximate position has been sketched in Figures 6c,d, although in this region the spherical bubble representing the HI shell has been disturbed due to the interaction with the cloud complex).

Discussing the HII and IR structures at $(l,b)=(351°,18°)$ and taking into account the presence of a strong UV field, de Geus concluded that part of the Rho Oph molecular cloud that was originally located in this region has been photodissociated after the passage of the shock front. A similar conclusion can be drawn on the structures around $(l,b)=(350°,22°)$: a photodissociated

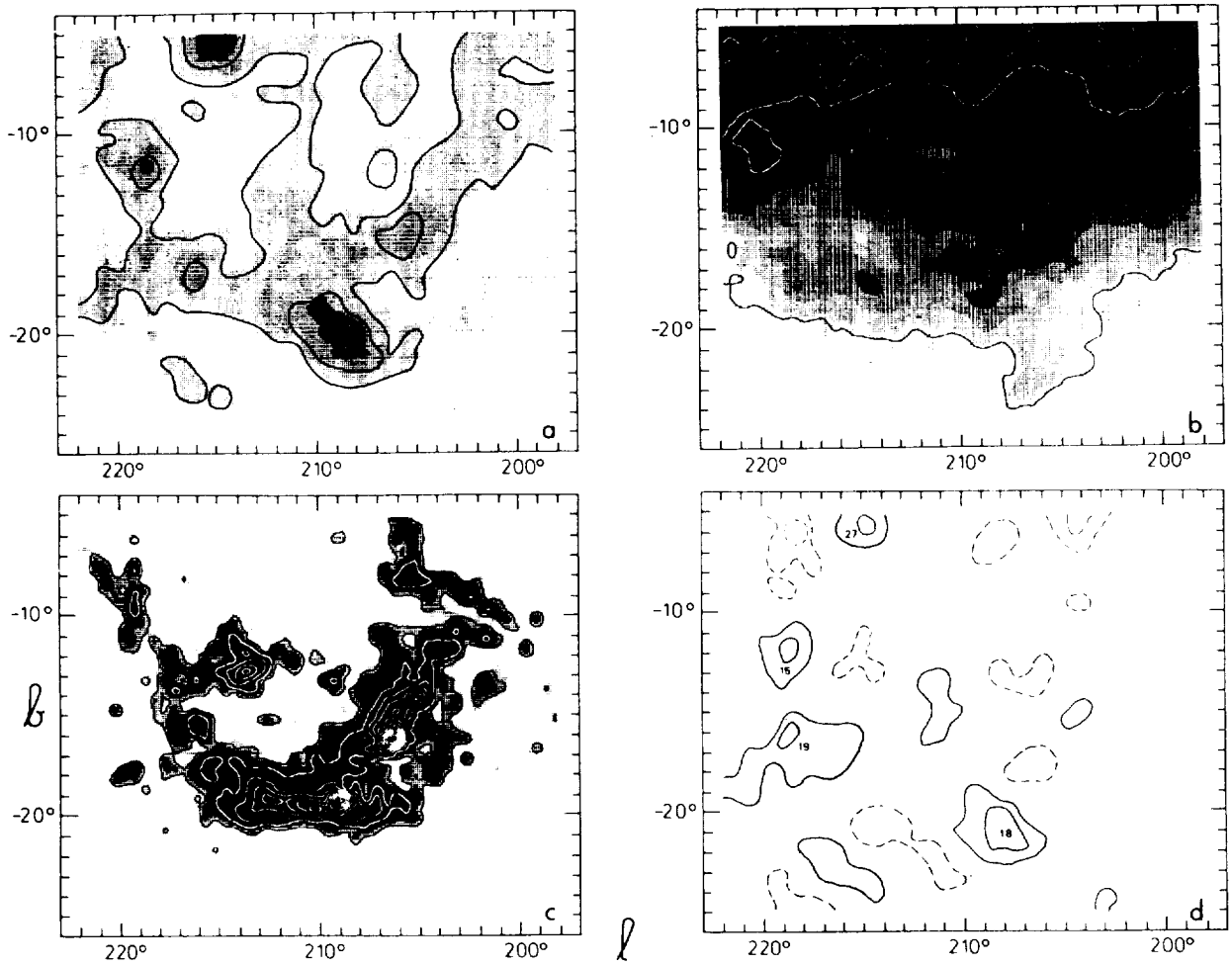

Fig. 7. The Orion-Monoceros region (from Bloemen et al. 1984; see there for additional explanation): a) Gamma-ray intensities in the 100-5000 MeV energy range. b) Total HI column densities. c) Velocity-integrated CO antenna temperatures W(CO). d) Map of the differences between the observed and the expected intensities. The gray areas and the full contours indicate positive excesses; the white regions and the dashed contours indicate deficiencies.

remnant of a molecular cloud. Blandford and Cowie (1982) discussed the scenario of a dense cloud overtaken by a strong supernova blast wave, in which dissociated molecules behind the shock, in a medium of enhanced gas and magnetic field density, are predicted to show up in gamma rays. However, this case seems to be different in that the SN-cloud interaction triggered star formation, and that the young stars apparently dissociated the gas clouds.

The important question arises: Do we need an enhancement in CR density inside this shell structure to explain the excess gamma-ray flux? Taking the preliminary mass estimates by de Geus, an enhancement in CR density of about an order of magnitude would be required to explain each of the excesses. It is unlikely that a CR enhancement in these dissociated molecular clouds originates

from the interaction described by Blandford and Cowie (1982), because, the CO complex is also overtaken by the shock, while no CR enhancement is found in the molecular clouds, but would then be expected.

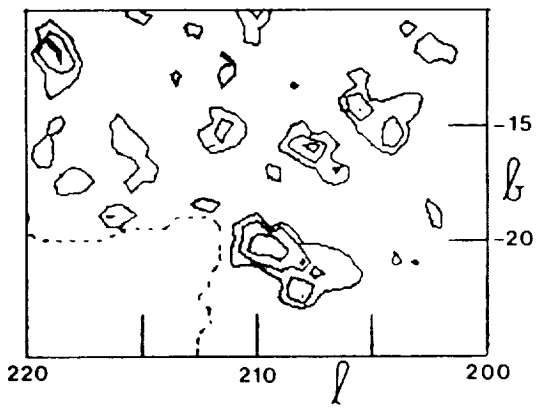

Fig. 8. Map of differences between the observed and predicted diffuse emission similar to Fig. 6d (see there for energy range and contour levels). Dashed line gives limit of exposure. The CO coverage is complete over this area. Not all excesses are significant; the excess at l=209° might be the only significant one.

Orion-complex region. Cowie, Songaila and York (1979) analysed UV absorption-line measurements for stars in or near the Orion OB1 and the λ Orionis associations, and interpreted their results together with those from previous 21-cm and visual absorption-line measurements. Very much similar to the findings of the Geus for the Ophiuchus region, they found highly ionized cloud material, which must be photo ionized by radiation from the young neighbouring Ori OB1 stars. Furthermore, they suggested that the observed gas features are caused by the effects of a recent supernova and of multiple supernovae, stellar winds and rocket-accelerated clouds, in combination with ionization by the association stars.

More recently, Bally et al. (1987) presented a large-scale ^{13}CO map of the Orion molecular cloud and concluded also that the morphology may be the consequence of the formation and evolution of the Ori OB1 association centered north of the molecular cloud. Similarly to the situation for Ophiuchus, the adjacent gamma-ray excess at about (l,b)=(209°,-21°) is located in a dense HII region on the side of the cloud facing the Ori OB1 association, so that part of the cloud that first experienced the interaction with the shock front (or superbubble) that overtook and shaped the cloud complex.

An alternative explanation for the gamma-ray excesses adjacent to the Ophiuchus and Orion cloud complexes is the production of Inverse Compton gamma rays due to electron-photon interactions in enhanced photon fields around the early type stars. However, these stars ionized the ISM locally, and it seems difficult to maintain the required enhancements in photon density together with some enhancement in electron density in the ionized medium around the stars, to explain the gamma-ray excesses. More accurate experimental data is required, such as more detailed mass estimates, and better spectral information in the gamma-ray domain. The Soviet-French Gamma-1 mission, and the NASA GRO

mission will provide more accurate spatial and energy distributions which might help discriminating the different possible production mechanisms.

References
Bally, J. et al., 1987, Ap. J. Letters, **312**, L45.
Bignami, G.F. et al., 1988, Astr. Ap., **202**, L1.
Blandford, R.D., Cowie, L.L., 1982, Ap. J. **260**, 625.
Bloemen, J.B.G.M. et al., 1984, Astr. Ap., **139**, 37.
Bloemen, J.B.G.M., 1989, Ann. Rev. of Astr. Ap., **27**.
Clear J. et al., 1988, Astr. Ap., **174**,85.
Cowie, L.L.,Songaila, A., York, D.G., 1979, Ap. J., **230**, 469.
De Geus, E.J., 1988, Ph.D. Thesis, Leiden University.
Grenier I.A. et al., 1988, Astr. Ap., **204**, 117.
Grenier, I.A., Hermsen, W., Hote, C., 1990, in Proc. XXI ICRC, Adelaide.
Halpern J.H. and Tytler D., 1988, Ap. J., **330**, 201.
Hermsen, W., 1980, Ph.D. Thesis, Leiden University.
Hermsen, W., Bloemen, J.B.G.M., 1983, "Surveys of the Southern Galaxy", eds. W.B. Burton, F.P. Israel, p. 65, Reidel Publ. Comp.
Hermsen, W., Spoelstra, T.A.Th., 1990, Proc. XXI ICRC, Adelaide.
Masnou et al., 1981, Proc. XVIIth ICRC, Paris, **1**, 177.
Mayer-Hasselwander, H.A. and Simpson, G., 1988, "Advances and perspectives in X-ray and gamma-ray astronomy" eds. J.A.M. Bleeker, W. Hermsen, Advances in Space Research, Vol. 10, Nr. 2, 89, Pergamon Press.
Morfill, G.E. et al., 1981, Ap. J. **246**, 810.
Pollock et al.,1985a, Astr. Ap., **146**, 352-362.
Pollock et al.,1985b, 19th ICRC, La Jolla, **1**, 338-341.
Pollock, A.M.T., Hermsen, W., 1990, in Proc. XXI ICRC, Adelaide.
Simpson, G., Mayer-Hasselwander, H.A., 1987, XX ICRC, Moscow, **1**, 89.
Ruderman M. and Cheng K.S., 1988, Ap. J., **335**, 306.
Spoelstra, T.A.Th. and Hermsen, W., 1984, Astr. Ap. **135**, 135.
Sieber, W. and Schlickeiser, R., 1982, Astr. Ap. **113**, 314.
Strong et al., 1987, Astr. Ap. Suppl., **67**,283.
Strong et al., 1988, Astr. Ap., **207**, 1-15.
Swanenburg et al., 1981, Ap. J. Letters, **243**, L69.
Thompson et al., 1977, Ap. J. Letters, **214**, L17.
Wouterloot, J.G.A., 1981, Ph.D. Thesis, Leiden University.

DISCUSSION

John Mattox:

Is it possible to include the spectral break point in the maximum likelihood analysis of Geminga?

Wim Hermsen:

It is possible, but CPU-time consuming. What we can do now is to compare the maximum likelihood values for the different selected break energies. This will give already a clear indicator which break energy is favored by the data.